Neuron 50, 465–477, May 4, 2006 ©2006 Elsevier Inc. DOI 10.1016/j.neuron.2006.03.041

A Clock Shock: Mouse CLOCK Is Not Required for Circadian Oscillator Function

Jason P. DeBruyne,[1] Elizabeth Noton,[1,3] Christopher M. Lambert,[1] Elizabeth S. Maywood,[2] David R. Weaver,[1,*] and Steven M. Reppert[1]
[1] Department of Neurobiology
University of Massachusetts Medical School
364 Plantation Street
Worcester, Massachusetts 01605
[2] Medical Research Council
Laboratory of Molecular Biology
Neurobiology Division
Hills Road
Cambridge CB2 2QH
United Kingdom

Summary

The circadian clock mechanism in the mouse is composed of interlocking transcriptional feedback loops. Two transcription factors, CLOCK and BMAL1, are believed to be essential components of the circadian clock. We have used the *Cre-LoxP* system to generate whole-animal knockouts of CLOCK and evaluated the resultant circadian phenotypes. Surprisingly, CLOCK-deficient mice continue to express robust circadian rhythms in locomotor activity, although they do have altered responses to light. At the molecular and biochemical levels, clock gene mRNA and protein levels in both the master clock in the suprachiasmatic nuclei and a peripheral clock in the liver show alterations in the CLOCK-deficient animals, although the molecular feedback loops continue to function. Our data challenge a central feature of the current mammalian circadian clock model regarding the necessity of CLOCK:BMAL1 heterodimers for clock function.

Introduction

Endogenous circadian clocks drive daily rhythms of physiology and behavior in most organisms. In mammals, circadian clocks operate in nearly all cells and tissues and are organized hierarchically (Reppert and Weaver, 2002; Lowrey and Takahashi, 2004). At the top of this hierarchy is a master clock that resides within the suprachiasmatic nuclei (SCN) of the anterior hypothalamus. The SCN clock is entrained to the 24 hr period by the daily light-dark cycle acting through retina to SCN pathways, and, in turn, the entrained SCN synchronizes the phase of circadian oscillators in peripheral tissues. Peripheral oscillators drive the rhythmic expression of genes involved in the physiological processes carried out by that tissue (see Duffield, 2003; Lowrey and Takahashi, 2004).

The intracellular molecular mechanism underlying the mammalian clockwork has been most extensively studied in the mouse, where interlocking transcriptional feedback loops drive the self-sustaining clock mechanism in both the SCN and peripheral tissues (Shearman et al., 2000; Lowrey and Takahashi, 2004; Reppert and Weaver, 2002). At the core of the molecular clock lies a pair of PAS-containing bHLH transcription factors, CLOCK and BMAL1. CLOCK:BMAL1 heterodimers drive the rhythmic expression of three *Period* genes (*mPer1–mPer3*) and two *Cryptochrome* genes (*mCry1* and *mCry2*) through E box enhancer elements. The resultant proteins form PER/CRY complexes that translocate back into the nucleus to inhibit CLOCK:BMAL1-mediated transcription, completing the negative transcriptional feedback loop essential for clockwork function. Post-translational processes appear to contribute to the time delays in the feedback mechanism needed for a 24 hr clock (Lowrey et al., 2000; Lee et al., 2001, 2004). An interlocking positive transcriptional feedback loop involves CLOCK:BMAL1 heterodimers indirectly regulating a rhythm in *Bmal1* transcription; the nuclear orphan receptor genes *Rev-erbα* and *Rora* are coordinately activated by CLOCK:BMAL1 to produce proteins that compete for the same promoter element, but have opposing actions, on *Bmal1* transcription (Preitner et al., 2002; Ueda et al., 2002; Sato et al., 2004; Akashi and Takumi, 2005). The positive feedback loop may add stability to the core clock mechanism (Emery and Reppert, 2004).

Because of the hierarchical nature of the mammalian circadian timing system, we have begun to address circadian function in individual tissues by using the *Cre-LoxP* recombination system (Nagy, 2000; Morozov et al., 2003) to disrupt clock function in a tissue-specific manner. We chose to target the *Clock* gene because all available genetic, molecular, and biochemical data to date suggest that it is a critical component of the circadian clockwork (Lowrey and Takahashi, 2004). The genetic data come from analysis of mice carrying a dominant-negative, antimorphic *Clock* allele ($Clock^{\Delta 19}$) recovered in a mutagenesis screen (Vitaterna et al., 1994; Antoch et al., 1997; King et al., 1997a; 1997b). The mutant CLOCK protein lacks the residues encoded by exon 19 and competes with wild-type CLOCK in heterozygous animals (King et al., 1997a) and renders CLOCK:BMAL1 heterodimers functionally defective in the homozygous mutants (Gekakis et al., 1998; Jin et al., 1999). Homozygous *Clock* mutant mice ($Clock^{\Delta 19/\Delta 19}$) have a long circadian period (26–28 hr in length, which can degenerate to arrhythmicity, depending on genetic background (Vitaterna et al., 1994; Oishi et al., 2002; Kennaway et al., 2003; Ochi et al., 2003) and markedly blunted molecular rhythms in the SCN (Jin et al., 1999; Kume et al., 1999; Oishi et al., 2000; Ripperger et al., 2000; Cheng et al., 2002). Furthermore, mice homozygous for a null allele of *Bmal1* have disrupted behavioral and molecular rhythms (Bunger et al., 2000).

In the present report, we used the *Cre-LoxP* system to disrupt the *Clock* gene and analyzed the behavioral and molecular rhythms in these null mutant mice. To our surprise, CLOCK-deficient mice continue to express robust circadian rhythms in locomotor activity, but they do

*Correspondence: david.weaver@umassmed.edu
[3] Present address: Genome Damage and Stability Centre, University of Sussex, Falmer, Brighton, United Kingdom BN1 9RQ.

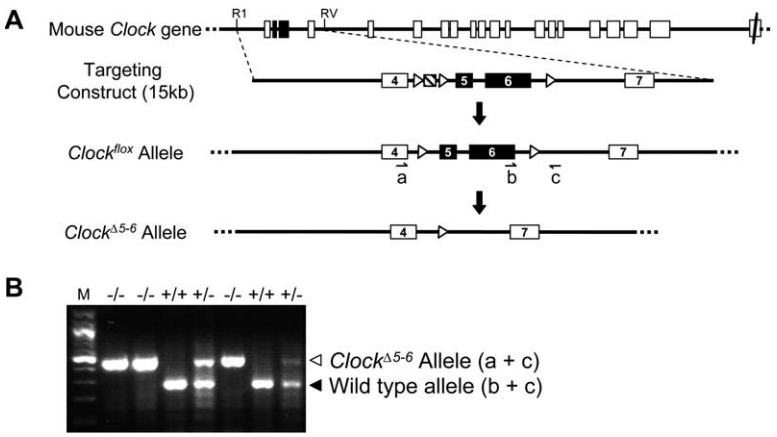

Figure 1. Generation of a Conditional *Clock* Allele

(A) Schematic representation of the mouse *Clock* gene, targeting construct, floxed allele (*Clock*^{flox}), and flox-deleted allele (*Clock*$^{\Delta 5\text{-}6}$). A 10 kb portion of the *Clock* gene was excised with *Eco*R1 (R1) and *Eco*RV (RV), and a dual neomycin resistance/thymidine kinase selection cassette (hatched box), flanked by *LoxP* sites (arrowheads), was inserted between exons 4 and 5. An additional *LoxP* site was inserted between exons 6 and 7. Boxes represent exons, and the lines between the boxes indicate introns. The black boxes represent the floxed (targeted) exons. The small arrows (a–c) show the location and direction of primers for PCR genotyping.

(B) PCR genotyping of DNA extracted from mouse tails of offspring from pairing of heterozygous *Clock* deletion mutant mice (*Clock*$^{+/\Delta 5\text{-}6}$). Primers a plus c amplify the *Clock*$^{\Delta 5\text{-}6}$ allele (−), while primers b plus c amplify the wild-type allele (+). Primer sequences: a, 5′-CAGCTTCATTTGAAATCTGCAT-3′; b, 5′-AGCTGGGGTCTATGCTTCCT-3′; c, 5′-CGCTGAGAGCCAAGACAAT-3′. Genotypes are shown above lanes. M, size marker (100 bp ladder, NEB).

have altered responses to light. At the molecular and biochemical levels, clock gene mRNA and protein levels in both the SCN and liver show several alterations in the null mutant animals, but the molecular clock continues to run. Our data indicate that a central tenet of the mammalian circadian clock model, the necessity of CLOCK:BMAL1 heterodimers for clockwork function, needs to be reassessed.

Results and Discussion

Generation of a Conditionally Disrupted Allele of *Clock*

To generate mice carrying an allele of *Clock* that can be conditionally disrupted, we used a "knockin" gene targeting approach to introduce *LoxP* sites into the introns flanking exons 5 and 6; these exons encode the bHLH domain, which appears to be required for CLOCK interaction with BMAL1 (Rutter et al., 2001), as well as its nuclear translocation (Kondratov et al., 2003). The 15 kb targeting construct (Figure 1A) carried two selectable markers, neomycin (Neo) resistance and thymidine kinase (TK), flanked by *LoxP* sites between exons 4 and 5, and an additional *LoxP* site between exons 6 and 7. ES cells were transfected with this targeting construct, and 22 of 384 neomycin-resistant clones had probable homologous integration as determined by restriction digest and Southern blot analysis (data not shown). Two of the ES clones were subsequently transfected with *Cre recombinase* (*Cre*) to remove the Neo-TK markers, and subclones were selected for the absence of TK using gancyclovir. The polymerase chain reaction (PCR) was used to screen for subclones in which recombination led to excision of the floxed Neo-TK cassette and retention of exons 5–6 flanked on each side by a single *LoxP* site (Figure 1A; *Clock*^{flox} allele). Two of these subclones, confirmed to contain the floxed allele by Southern blot analysis and long-range genomic PCR, were injected into C57BL/6J blastocysts. Twenty-seven chimeric mice were recovered and bred with C57BL/6J mice. One of the ~600 pups born received the *Clock*^{flox} allele. This mouse served as the founder to establish a line of *Clock*^{flox} mice.

Because a *Clock* null mutation has not been previously reported, we crossed the *Clock*^{flox} line to a transgenic line expressing *Cre* under the control of the *Protamine1* promoter (*PRM1-Cre*; O'Gorman et al., 1997) (Figure 1A, *Clock*$^{\Delta 5\text{-}6}$ allele). In *PRM1-Cre* mice, *Cre* is expressed in the testis, inducing a recombination between *LoxP* sites in male germ cells; thus exons 5 and 6 were deleted during spermatogenesis, and the recombined *Clock*$^{\Delta 5\text{-}6}$ allele was passed to the offspring from the male parent. Heterozygous whole-animal *Clock* deletion mutant mice (*Clock*$^{+/\Delta 5\text{-}6}$) were identified and crossed. Heterozygote intercrosses produced progeny of each genotype (Figure 1B) in the expected 1:2:1 ratios (26.0% wild-type, 48.7% heterozygous, 25.3% homozygous; n = 454 offspring), indicating that animals homozygous for this deletion mutation are viable. Homozygous *Clock*$^{\Delta 5\text{-}6/\Delta 5\text{-}6}$ mutant mice had no gross anatomical abnormalities.

Clock$^{\Delta 5\text{-}6}$ Is a Null Allele

We used previously characterized antibodies generated against the C-terminal portion of the CLOCK protein (Lee et al., 2001) to determine whether the deletion of exons 5 and 6 of *Clock* allowed production of a protein product. Using an antibody generated in guinea pigs (gp), prominent nuclear immunostaining was detected in the SCN of wild-type mice, and nuclear immunostaining was absent in the homozygous *Clock*$^{\Delta 5\text{-}6/\Delta 5\text{-}6}$ mutant mice (Figure 2A, left). Diffuse staining was also observed in a population of glial-like cells in both wild-type mice and homozygous *Clock*$^{\Delta 5\text{-}6/\Delta 5\text{-}6}$ mutant mice (Figure 2A, left). Using an antibody to the same epitope of CLOCK generated in rats, however, only nuclear staining was observed in wild-type mice, and this staining was absent in the SCN of *Clock*$^{\Delta 5\text{-}6/\Delta 5\text{-}6}$ mutant mice (see Figure S1 in the Supplemental Data available online). This indicates that the glial-like staining seen with CLOCK-gp was nonspecific and does not represent CLOCK protein. We conclude that the deletion mutation is indeed a null; homozygous *Clock*$^{\Delta 5\text{-}6/\Delta 5\text{-}6}$ mutant mice are therefore subsequently referred to as *Clock*$^{-/-}$ or CLOCK-deficient mice. BMAL1 immunoreactivity in the SCN of the *Clock*$^{-/-}$ mice was reduced by >90% (Figure 2A, right).

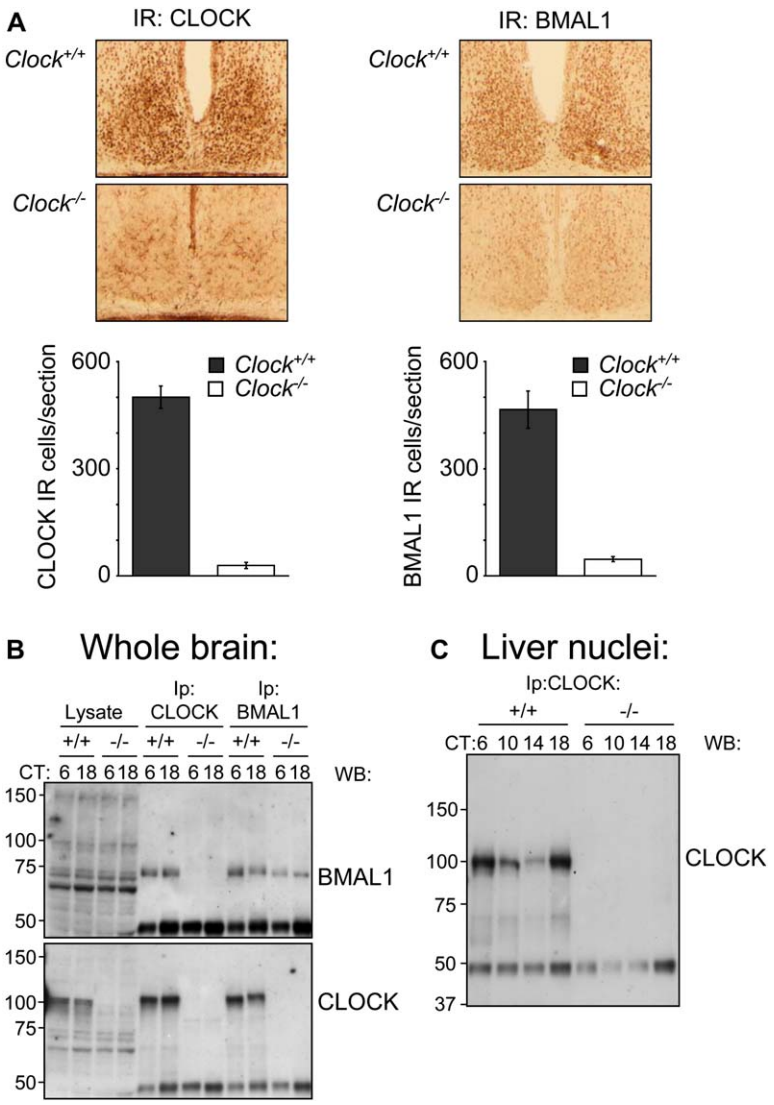

Figure 2. Deletion of Exons 5 and 6 Results in a Null *Clock* Allele

(A) Immunohistochemical confirmation of CLOCK deficiency in the SCN. The photomicrographs show immunoreactivity (IR) for CLOCK (left) or BMAL1 (right) in adjacent coronal sections of the SCN from wild-type (*Clock*$^{+/+}$) or homozygous *Clock*$^{-/-}$ mutant mice collected at zeitgeber time (ZT) 8. The histograms below the photomicrographs depict the mean ± SEM of the number of immuno-positive cells for four animals per genotype. CLOCK and BMAL1 immunoreactivity were significantly reduced in the SCN of *Clock*$^{-/-}$ mutant animals compared to wild-type mice ($p < 0.0005$; t test). The remaining CLOCK-immunopositive cells in the *Clock*$^{-/-}$ mice are glial-like cells, rather than nuclei, and these cells were not observed with another CLOCK antibody (Figure S1).

(B) Biochemical confirmation of CLOCK deficiency in brain. Brains were collected from wild-type (*Clock*$^{+/+}$) and homozygous *Clock*$^{-/-}$ mutant mice at circadian time (CT) 6 and 18 on the first day in constant darkness. The brains were homogenized, and the lysates were immunoprecipitated (Ip) with antibodies against CLOCK or BMAL1. The immune complexes were Western blotted (WB) and probed for either BMAL1 (upper) or CLOCK (lower). The migration positions of protein size standards (in kilodaltons) are shown on the left. The blots are representative of two experiments.

(C) Biochemical confirmation of CLOCK deficiency in liver. Nuclei were purified from four livers collected from wild-type (*Clock*$^{+/+}$) or homozygous *Clock*$^{-/-}$ mutant mice at CT 6, 10, 14, and 18 on the first day in constant darkness. The nuclei were immunoprecipitated (Ip) with an antibody against CLOCK, and the immune complexes were Western blotted and probed for CLOCK. The migration positions of protein size standards (in kilodaltons) are shown on the left.

Immunoprecipitation (IP) experiments of whole-brain lysates (Figure 2B) and liver nuclear extracts (Figure 2C) confirmed that the remaining immunoreactivity in *Clock*$^{-/-}$ mice was nonspecific. The anti-CLOCK antibody precipitated CLOCK from wild-type mice, but failed to purify any protein in *Clock*$^{-/-}$ animals. Similarly, immunoprecipitation with anti-BMAL1 antibody failed to purify CLOCK in *Clock*$^{-/-}$ mice, but it did purify BMAL1 in both the wild-type and *Clock*$^{-/-}$ mice (Figure 2C, and data not shown). Taken together, these results demonstrate that the deletion of exons 5 and 6 of *Clock* results in a null allele, and mice homozygous for this allele are CLOCK deficient.

CLOCK-Deficient Mice Maintain Robust Locomotor Activity Rhythms

To determine the effect of CLOCK deficiency on behavioral rhythmicity, we monitored wheel-running activity under constant darkness (DD) for 4 weeks, following an initial 14 days in a 12 hr light/12 hr dark (LD) cycle. Consistent with a previous report that monitored behavioral rhythms in a strain heterozygous for a chromosomal deletion containing the *Clock* gene (King et al., 1997a), heterozygous *Clock* null mutant mice (+/−) displayed normal circadian patterns of behavior, with periods of 23.5 ± 0.2 hr (mean ± SEM; n = 8), similar to those of wild-type animals (+/+; 23.6 ± 0.1 hr; n = 17) (Figures 3A and 3B). CLOCK-deficient mice (−/−) maintained robust circadian patterns of behavior, with periodicities that were on average ~20 min shorter (23.2 ± 0.1 hr; n = 17) than their wild-type siblings (Figures 3A and 3B). All of the CLOCK-deficient mice tested displayed strong behavioral rhythmicity throughout the 4 weeks in DD, comparable to that of their wild-type siblings (Figures 3A and 3C), despite a slight reduction in their activity levels (Figure 3D). Thus, CLOCK is not required for the generation of robust circadian rhythms in locomotor activity.

CLOCK-Deficient Mice Have Altered Behavioral Responses to Light

When maintained on the LD cycle, mouse locomotor activity is typically restricted to the night via daily light-induced resetting of the underlying circadian pacemaker to maintain synchrony of the clock to the 24 hr day (termed "entrainment"). During the initial period of behavioral monitoring in LD, wild-type and heterozygous

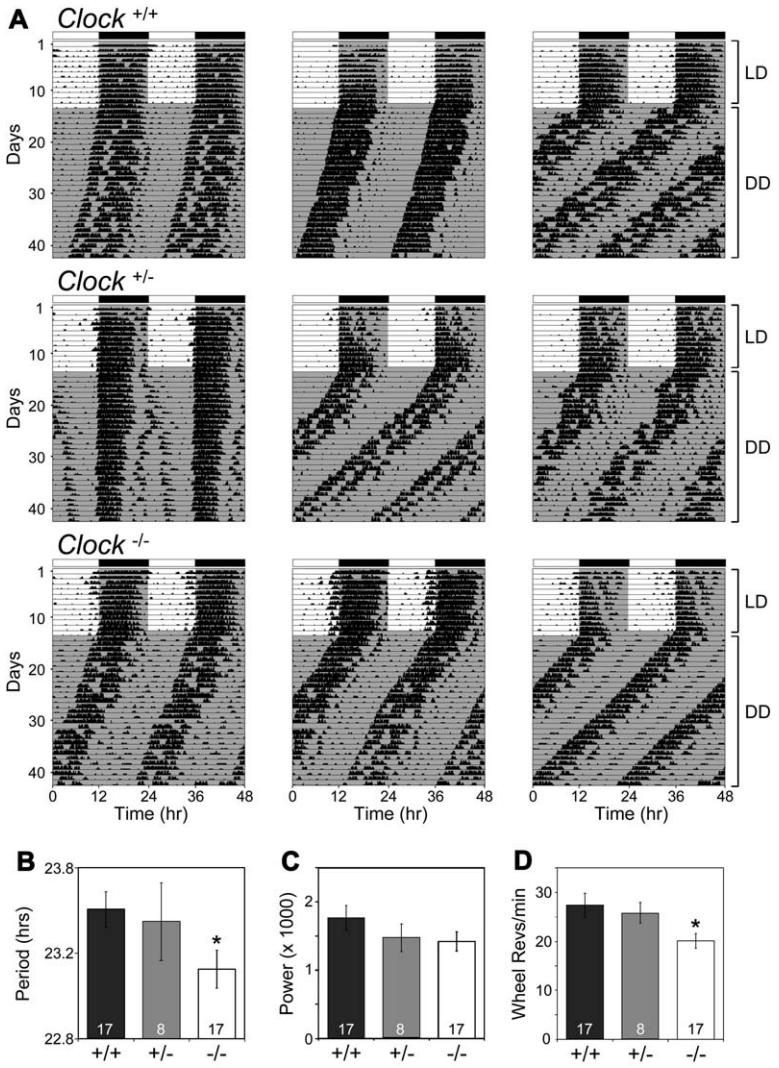

Figure 3. Locomotor Activity Rhythms Persist in CLOCK-Deficient Mice

(A) Representative activity records (actograms) of wild-type mice (*Clock*$^{+/+}$; top row), heterozygous *Clock* mutant mice (*Clock*$^{+/-}$; center row), and CLOCK-deficient mice (*Clock*$^{-/-}$; lower row) are shown in double-plotted format. Each horizontal line represents 48 hr; the second 24 hr period is plotted to the right and below the first. Vertical bars represent periods of wheel-running activity. Animals were initially housed in a 12L:12D light-dark cycle (LD) and were then transferred to constant darkness (DD). The timing of the LD cycle is indicated by the bar above the top records. Numbers on the left indicate days of study.

(B) Periodogram estimates of period for each genotype. Each bar is mean ± SEM; the number of animals is indicated within each bar. *p = 0.03 compared with wild-type, t test.

(C) Circadian amplitude (power from periodogram analyses). The genotypes did not differ.

(D) Activity levels during the last 4 weeks of DD for each genotype. *p = 0.017 compared to wild-type (t test).

animals showed normally entrained daily patterns of activity, initiating their nightly bouts of activity at the beginning of the dark period (Figure 3A; data not shown). However, we noticed that most CLOCK-deficient animals became active ~2 hr before lights-off (Figure 3A), suggesting that they may have altered resetting responses to light. Alternatively, this advanced activity could be due to a deficit in the "masking" effect of light and not altered entrainment, as masking alterations have been shown in BMAL1-deficient (Bunger et al., 2000) and homozygous *Clock* mutant mice (Redlin et al., 2005). It should be noted, however, that upon re-entrainment to LD (see below), CLOCK-deficient mice initiated their activity coincident with lights-off, as observed in the other genotypes.

To examine resetting responses to light, wild-type, heterozygous, and CLOCK-deficient mice were exposed to LD for several weeks and then were exposed to a 4 hr extension of the light period, followed by constant darkness (Figure 4A). Exposure to light during this period of the night (zeitgeber time [ZT] 12–16) was expected to cause a phase delay in the activity rhythm (see Dunlap, 1999). Wild-type and heterozygous mutant mice responded as expected, with average (±SEM) delays of 1.6 ± 0.1 and 1.9 ± 0.5 hr, respectively. In contrast, the activity rhythm of CLOCK-deficient mice was not delayed by the 4 hr light extension (Figure 4A). To rule out the possibility that the apparent phase shifts after light exposure were due to an abnormal phase of entrainment, the phase of rhythmicity after release of the same animals directly into DD was assessed. Comparison of the phase of rhythmicity after release into DD with that after the light extension revealed that the phase shifts in the wild-type and heterozygous mice were statistically significant (paired t tests, $p < 0.05$), while those in the CLOCK-deficient mice were not (Figure 4A; $p = 0.7$).

The animals were subsequently re-entrained to LD12:12 for 3 weeks and were then exposed to a light stimulus expected to elicit a phase advance of the activity rhythm (see Dunlap, 1999). Specifically, following the last normal lighting cycle, animals were exposed to a single, 4 hr light pulse late in the night (at ZT 20–24), and then were released into constant darkness (see Figure 4B). Wild-type and heterozygous mutant mice responded with phase advances of 1.8 ± 0.5 and 2.0 ± 0.6 hr, respectively (Figure 4B). These phase advances were significantly greater than when the same animals were placed into DD without the light pulse ($p < 0.01$, paired

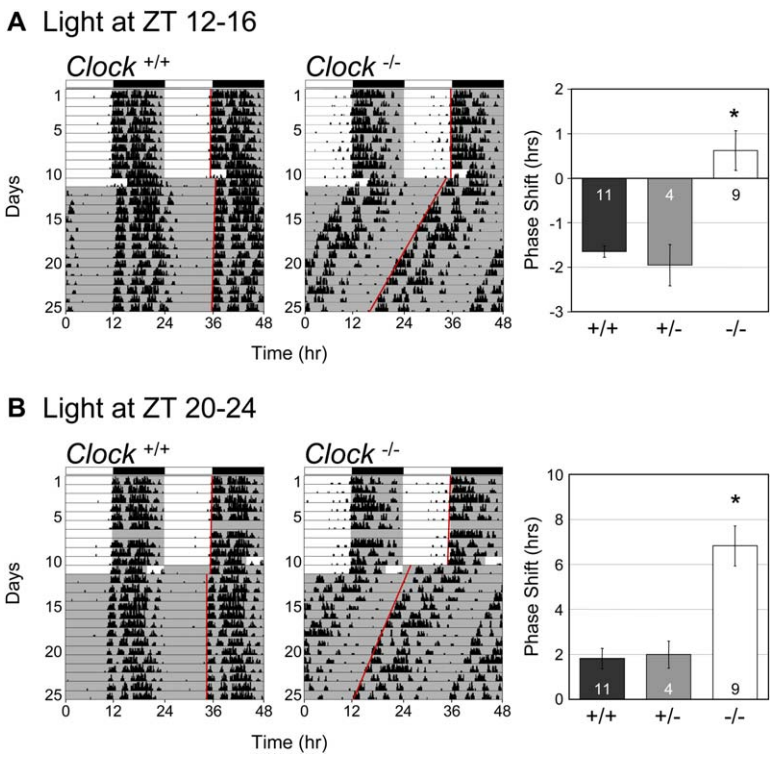

Figure 4. CLOCK-Deficient Mice Have Altered Behavioral Responses to Light

(A) Response to light from ZT 12–16. Double-plotted activity records (left) from a representative wild-type (*Clock*$^{+/+}$) and CLOCK-deficient (*Clock*$^{-/-}$) mouse. Animals were initially housed in a 12L:12D light-dark cycle (shown above the activity record). The lights were then left on from ZT 12–16, followed by exposure to constant darkness. The red lines delineate the phase of activity onset before and after the light manipulation. The bar graph at right shows mean ± SEM of the phase shifts for each genotype; numbers of animals for each group are shown below the zero line. Positive numbers are phase advances; negative numbers are phase delays. *p < 0.001 ANOVA, Sheffe's S post hoc test, compared to wild-type.

(B) Response to light from ZT 20–24. Double-plotted activity records (left) from a representative wild-type (*Clock*$^{+/+}$) and CLOCK-deficient (*Clock*$^{-/-}$) mouse. Animals were initially housed in a 12L:12D light-dark cycle (LD). The lights were then turned on from ZT 20–24, followed by exposure to DD. The red lines delineate the phase of activity onset before and after the light manipulation. The bar graph at right shows mean ± SEM of the phase shifts for each genotype; numbers of animals for each group are shown below the zero line. *p < 0.0001 ANOVA, Sheffe's S post hoc test, compared to wild-type.

t tests), indicating that the phase advances were light induced. Light-induced advances of the activity rhythm in CLOCK-deficient mice averaged 6.8 ± 0.9 hr, more than three times larger than those occurring in their wild-type and heterozygous siblings. These large phase advances in CLOCK-deficient mice are similar to those observed in REV-ERBα-deficient mice (Preitner et al., 2002).

These results indicate that CLOCK-deficient mice have altered responses to light, with reduced phase delays and exaggerated phase advances in the paradigms used. CLOCK may have a role in the light input pathway or in regulating SCN responsiveness to light. One potential mechanism for enhancing the magnitude of phase shifts is through reduction of pacemaker amplitude (Winfree, 1970), but this would not explain the failure of CLOCK-deficient mice to phase delay.

Molecular Rhythms in the SCN of CLOCK-Deficient Mice

Since CLOCK-deficient mice exhibit nearly normal circadian patterns of locomotor behavior, we predicted that the molecular oscillator driving circadian gene expression patterns in the master pacemaker in the SCN would not be dramatically affected in these mice. To test this prediction, brains were collected from wild-type and CLOCK-deficient mice at 4 hr intervals across the circadian cycle during the first day in DD and processed for in situ hybridization to determine the expression levels of the core clock genes *mPer1*, *mPer2*, *Rev-erb*α, and *Bmal1* (Figure 5A) and the clock-controlled genes (CCGs) *Pk2*, *Avp*, and *Dbp* (Figure 5B) in the SCN. We chose to examine these particular genes because, with the exception of *Bmal1*, all are putative direct targets of CLOCK:BMAL1-mediated transcription through E box enhancer elements (Gekakis et al., 1998; Jin et al., 1999; Ripperger et al., 2000; Cheng et al., 2002; Yoo et al., 2005; Ueda et al., 2005).

The *mPer1*, *mPer2*, *Rev-erb*α, and *mBmal1* genes all expressed significant circadian rhythms in mRNA levels in the SCN of wild-type mice (ANOVAs, $p < 0.01$), consistent with previous reports (Jin et al., 1999; Oishi et al., 2000, 2002; Shearman et al., 2000; Preitner et al., 2002). mRNA levels of these genes were also rhythmic in the SCN of CLOCK-deficient mice (ANOVAs, $p < 0.03$) (Figure 5A). However, in the absence of CLOCK, the amplitudes of the *mPer1*, *Rev-erb*α, and *Bmal1* rhythms were reduced compared to those in wild-type mice. In the CLOCK-deficient SCN, the peak mRNA levels of *mPer1* and *Rev-erb*α were reduced to about 50% of the wild-type levels, whereas the trough values were unchanged. The opposite effect was observed with *Bmal1* mRNA levels (Figure 5A). In the SCN of CLOCK-deficient mice, *Bmal1* mRNA was elevated during the subjective day, at near peak levels from CT 2–14 but then declined to trough levels by CT 22, while the profile in wild-type mice is characterized by low levels throughout the subjective day. The elevation in *Bmal1* expression in CLOCK-deficient SCN may be partially due to the reduced expression of the repressor, *Rev-erb*α (Preitner et al., 2002). mRNA levels of *mPer2* in the SCN of CLOCK-deficient mice, in contrast, were rhythmic with peak and trough values similar to wild-type values. The only alteration was that the peak of the *mPer2* rhythm in the CLOCK-deficient SCN occurred earlier than the rhythm in wild-type SCN (Figure 5A).

The mRNA levels of the CCGs *Pk2* and *Avp* were also expressed rhythmically in the SCN of CLOCK-deficient mice (ANOVAs, $p < 0.001$), and these rhythms were

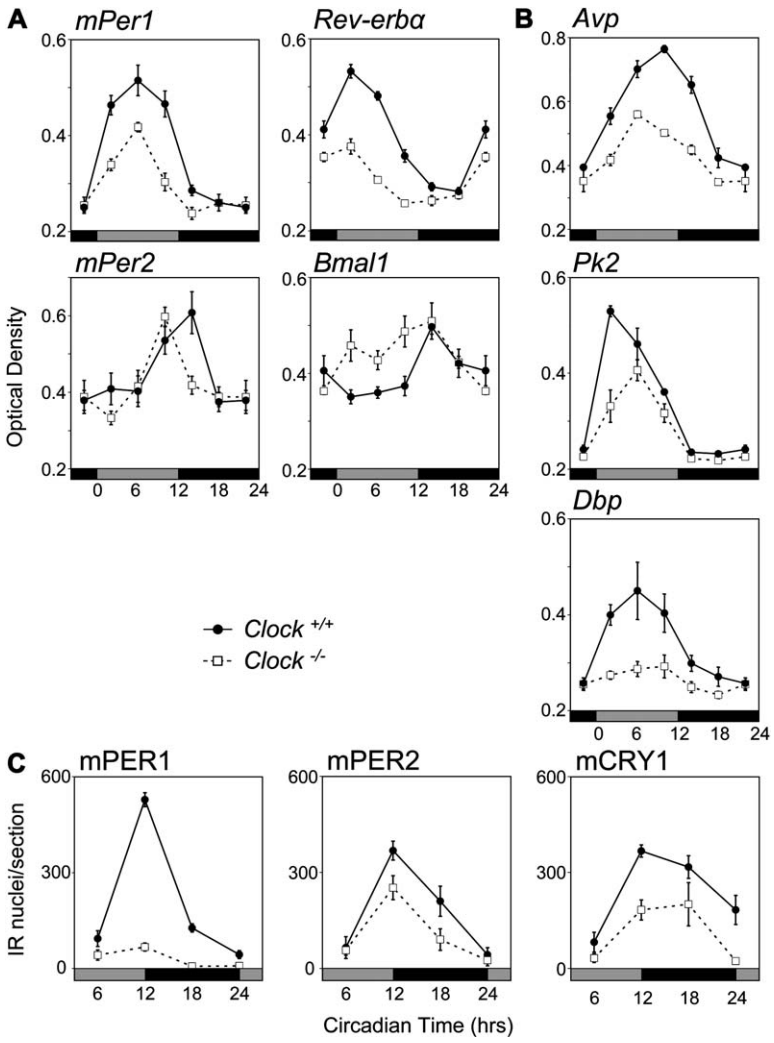

Figure 5. Gene Expression and Protein Patterns in the SCN

(A) Clock gene mRNA rhythms are altered in the SCN of CLOCK-deficient mice. Brains were collected from wild-type mice (*Clock*$^{+/+}$; solid lines) and CLOCK-deficient mice (*Clock*$^{-/-}$; dashed lines) at 4 hr intervals on the first day in DD, and the mRNA levels of *mPer1*, *mPer2*, *Rev-erbα*, and *Bmal1* were determined by in situ hybridization. Each point is the mean ± SEM of three to four animals. The horizontal bar at the bottom of each panel represents the lighting cycle that the animals experienced prior to placement in DD; day is gray, and night is black. Data from CT 22 are double plotted.

(B) Clock-controlled gene mRNA rhythms are altered in the SCN of CLOCK-deficient mice. The mRNA levels of *Avp*, *Pk2*, and *Dbp* were determined by in situ hybridization. Each point is the mean ± SEM of three to four animals. Data from CT 22 are double plotted.

(C) Clock protein levels oscillate in SCN nuclei at reduced amplitude in CLOCK-deficient mice. Nuclear staining for mPER1, mPER2, and mCRY1 in the SCN are depicted for wild-type mice and CLOCK-deficient mice. For each antigen, values are mean ± SEM of three to five animals at 6 hr intervals on the first day in DD. The markedly reduced rhythm in the number of mPER1-immunoreactive nuclei was confirmed in another experiment with 3 hr sampling intervals (data not shown).

also damped compared to wild-type mice (Figure 5B). In contrast, *Dbp* mRNA levels were low throughout the circadian day in the SCN of CLOCK-deficient mice (Figure 5B), and the mRNA levels did not exhibit a significant circadian oscillation (ANOVA, $p = 0.06$).

We also examined the rhythmicity of mPER1, mPER2, and mCRY1 protein accumulation in the SCN of wild-type and CLOCK-deficient mice using immunocytochemistry (Figure 5C). The results obtained for each protein from wild-type animals were similar to previous findings, with a prominent peak in nuclear staining at CT 12 (Hastings et al., 1999; Kume et al., 1999; Field et al., 2000). In the SCN of CLOCK-deficient mice, the number of mPER1 immunoreactive nuclei was rhythmic with a peak at CT 12 (ANOVA, $p \leq 0.01$), but peak levels were substantially reduced compared to wild-type at CT 12. The number of mPER2 and mCRY1 immunoreactive nuclei was also rhythmic in the SCN of CLOCK-deficient mice (ANOVA, $p \leq 0.01$ for each). The total number of positive nuclei for each protein near the peak (CT 12–18) was reduced compared to wild-type, although the effect of CLOCK deficiency on mPER2 and mCRY1 was much less than the effect on mPER1.

Overall, our data indicate that the CLOCK protein is not required for rhythmic gene expression within the SCN. However, CLOCK does appear to contribute to the amplitude of rhythmic gene expression in a gene-dependent manner. For the majority of genes examined (*mPer1*, *Rev-erbα*, *Pk2*, and *Avp*), CLOCK seems to contribute to maximal peak expression levels, adding robustness to their circadian expression patterns. The loss of CLOCK does not significantly impair *mPer2* expression and yet is required for circadian expression of *Dbp.* This shows that the contribution of CLOCK to circadian gene expression is target dependent.

Molecular and Biochemical Rhythms in the Liver of CLOCK-Deficient Mice

Oscillators in peripheral tissues such as the liver have been useful for understanding the biochemical and transcriptional mechanisms underlying circadian gene expression (e.g., Ripperger et al., 2000; Lee et al., 2001, Etchegaray et al., 2003; Preitner et al., 2002). Moreover, the general circadian clock mechanism is felt to be very similar between the SCN and the liver and other peripheral oscillators (Nagoshi et al., 2004; Welsh et al., 2005). We therefore compared gene expression profiles in the livers of wild-type and CLOCK-deficient mice. Livers were harvested from wild-type and CLOCK-deficient animals at 4 hr intervals across the first

day in DD, and gene expression levels were determined using TaqMan real-time PCR.

In wild-type mice, the mRNA patterns for each of the genes tested in the liver were similar to those previously reported (Figure 6A) (Oishi et al., 2000; Lee et al., 2001, Preitner et al., 2002). The profiles in CLOCK-deficient mice were altered in a gene-specific manner. *mPer1* mRNA levels in the livers of both wild-type and CLOCK-deficient mice expressed a significant circadian rhythm ($p = 0.005$, ANOVA), with peak levels at CT 10–14 (Figure 6A). However, the amplitude of the *mPer1* mRNA rhythm in CLOCK-deficient livers was considerably damped compared to wild-type (~5 fold versus ~20 fold, respectively; see Figure S2). Surprisingly, absolute levels of *mPer1* mRNA levels were elevated in the livers of CLOCK-deficient mice (ANOVA, main effect of genotype, $p < 0.001$), unlike the situation in the SCN.

mPer2 mRNA levels were robustly rhythmic in wild-type livers, but less obviously rhythmic in CLOCK-deficient livers (Figure 6A) (ANOVA, $p = 0.007$ and 0.04, respectively). In both genotypes, *mPer2* levels peaked at CT 14. The amplitude of the *mPer2* mRNA rhythm in CLOCK-deficient livers was reduced compared to wild-type livers (~4 fold versus ~12 fold, respectively; see Figure S2) due to the elevation of trough levels during the early subjective day (Figure 6A).

Rev-erbα mRNA levels were at low levels throughout the day in CLOCK-deficient livers, yet there was a statistically significant rhythm ($p = 0.003$, ANOVA) that peaked at ~CT 2 (about 8 hr earlier than in wild-type). However, the amplitude of the mRNA rhythm was only about 8-fold, compared to the ~70-fold change in wild-type livers. The impact of CLOCK deficiency on *Rev-erbα* mRNA levels in liver appeared greater than in the SCN (Figure 5A).

In CLOCK-deficient livers, *Bmal1* mRNA levels were expressed at constitutive high levels that were above wild-type peak levels (Figure 5A). The elevated mRNA levels are most readily explained by the reduced *Rev-erbα* expression in CLOCK-deficient livers, as the elevated *Bmal1* mRNA levels in CLOCK-deficient mice are very similar to those reported in livers from REV-ERBα-deficient mice (Preitner et al., 2002).

The expression of *mCry1* mRNA was robustly rhythmic in wild-type livers (ANOVA, $p = 0.002$). In CLOCK-deficient livers, *mCry1* mRNA levels were expressed near wild-type peak levels throughout the day. ANOVA did reveal a statistical difference in expression levels among the time points ($p = 0.006$, ANOVA), but post hoc analyses revealed an unusual, bimodal pattern of expression with peaks at CT 2 and CT 14. The expression of *mCry2* mRNA was not rhythmic in either wild-type or CLOCK-deficient livers, and overall expression levels were similar between the two genotypes (Figure S2B).

Dbp mRNA levels were expressed at extremely low levels in CLOCK-deficient livers (Figure 6A). There was a statistically significant rhythm (ANOVA, $p = 0.01$), with peak levels at CT 6, but its amplitude in CLOCK-deficient livers was only about ~5 fold, compared to the >250-fold rhythm in wild-type mice. This finding is similar to what we found in the SCN of CLOCK-deficient mice and suggests that the expression of *Dbp* is largely dependent on CLOCK in both tissues. Overall, our studies suggest that the amplitude of circadian gene

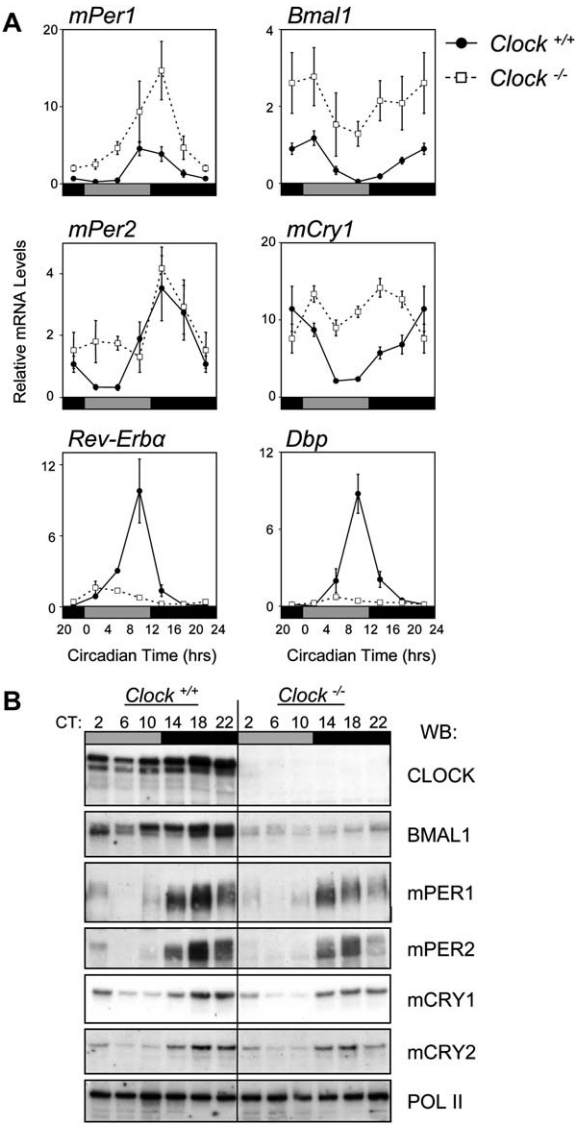

Figure 6. Gene Expression and Nuclear Protein Accumulation Patterns in the Liver

(A) Clock gene mRNA rhythms are altered in the liver of CLOCK-deficient mice. Livers were collected from wild-type mice (*Clock*$^{+/+}$; solid lines) and CLOCK-deficient mice (*Clock*$^{-/-}$; dashed lines) at 4 hr intervals on the first day in DD, and the mRNA levels of *mPer1*, *mPer2*, *Rev-erbα*, *Bmal1*, *mCry1*, and *Dbp* were determined by quantitative real-time PCR. Each point is the mean ± SEM of three to four animals. Data from CT 22 are double plotted. The horizontal bar at the bottom of each panel represents the lighting cycle that the animals experienced prior to placement in DD; day is gray, and night is black.

(B) Oscillations in clock protein levels in liver nuclei. Nuclei were processed from livers collected from wild-type (*Clock*$^{+/+}$) and homozygous *Clock*$^{-/-}$ mutant mice at CT 2, 6, 10, 14, 18, and 22 on the first day in constant darkness. The nuclear extracts from both genotypes were Western blotted (WB) simultaneously and probed for CLOCK, BMAL1, mPER1, mPER2, mCRY1, and mCRY2. The migration position of protein size standards (in kilodaltons) are shown on the left. Equal loading across lanes was confirmed by inspection of the intensities of nonspecific bands or Western blotting with RNA polymerase II antibodies (POL II). The blot is representative of two collections. The left and right halves of each blot were processed, probed, and exposed to film simultaneously for each antibody, and thus are directly comparable.

expression is significantly damped in the livers of CLOCK-deficient mice.

To obtain a clearer picture of clock mechanisms, we assayed the rhythmic translocation of clock proteins into the nucleus of both wild-type and CLOCK-deficient livers. Levels of mPER1, mPER2, mCRY1, and mCRY2 were rhythmic in the nuclei of CLOCK-deficient livers, being present during the subjective night and undetectable during the subjective day (Figure 6B) in a pattern similar to wild-type mice. Since the accumulation of the mPER proteins is rate limiting for this process (Lee et al., 2001), these data suggest that the relatively damped rhythms of *mPer1* and *mPer2* expression in the livers of CLOCK-deficient mice are still sufficient to rhythmically drive the mPER:mCRY repressor complex into the nucleus.

Nuclear mBMAL1 levels were substantially reduced in liver in the absence of CLOCK, despite its elevated mRNA expression, relative to wild-type (Figures 6A and 6B). This is consistent with our observations in the SCN (see Figure 2A) showing greatly reduced nuclear BMAL1 levels in the absence of CLOCK. Also, the rhythm in phosphorylated forms of mBMAL1 levels was not readily apparent without CLOCK (Figure 6B). These data indicate that, although mBMAL1 is required for nuclear entry of CLOCK, mBMAL1 can enter the nucleus without CLOCK, albeit at lower levels (Kondratov et al., 2003).

NPAS2: A Functional Replacement for CLOCK?

BMAL1-deficient mice lack detectable circadian clock function at both the molecular and behavioral levels (Bunger et al., 2000), and BMAL1 is felt to be the major partner for CLOCK (Reppert and Weaver, 2002; Lowrey and Takahashi, 2004). Our results with CLOCK-deficient mice suggest that there is another BMAL1 partner that can partially fulfill the functions of CLOCK within the circadian oscillator. The most likely candidate is Neuronal PAS domain protein 2 (NPAS2; also known as MOP4) (Hogenesch et al., 1997; Zhou et al., 1997). The mouse CLOCK and NPAS2 proteins are both paralogs of *Drosophila* CLOCK, and they share extensive sequence homology with each other, particularly within the bHLH and PAS domains (King et al., 1997b). In fact, several in vitro experiments indicate that NPAS2 can form transcriptionally active complexes with BMAL1 (Hogenesch et al., 1998; Kume et al., 1999; McNamara et al., 2001; Reick et al., 2001), and studies of NPAS2 mutant mice ($Npas2^{m/m}$) indicate that it is required for the circadian expression of *mPer2* mRNA levels in the forebrain (Reick et al., 2001).

We first determined whether NPAS2:BMAL1 heterodimers occur in vivo, using coimmunoprecipitation experiments. We incubated whole-brain extracts from wild-type and CLOCK-deficient mice harvested at CT 6 and 18, as well as from NPAS2-deficient mice collected during the daytime, with antibodies against BMAL1 and against NPAS2 (Lee et al., 2001; C. Lee and S.M.R., unpublished data), and probed subsequent immune complexes for NPAS2 and BMAL1. As shown in Figure 7A (upper panel), immunoprecipitation with NPAS2 antibodies successfully purified NPAS2 in both wild-type and CLOCK-deficient brains, as well as the truncated form of NPAS2 produced in the $Npas2^{m/m}$ mice (Garcia et al., 2000). Immunoprecipitation with BMAL1 antibodies also purified NPAS2 from wild-type and CLOCK-deficient brains, indicating that BMAL1:NPAS2 complexes occur in the brain, in vivo. Importantly, BMAL1 immune complexes from $Npas2^{m/m}$ brain extracts did not contain the truncated NPAS2 protein, verifying the specificity of this interaction. We subsequently

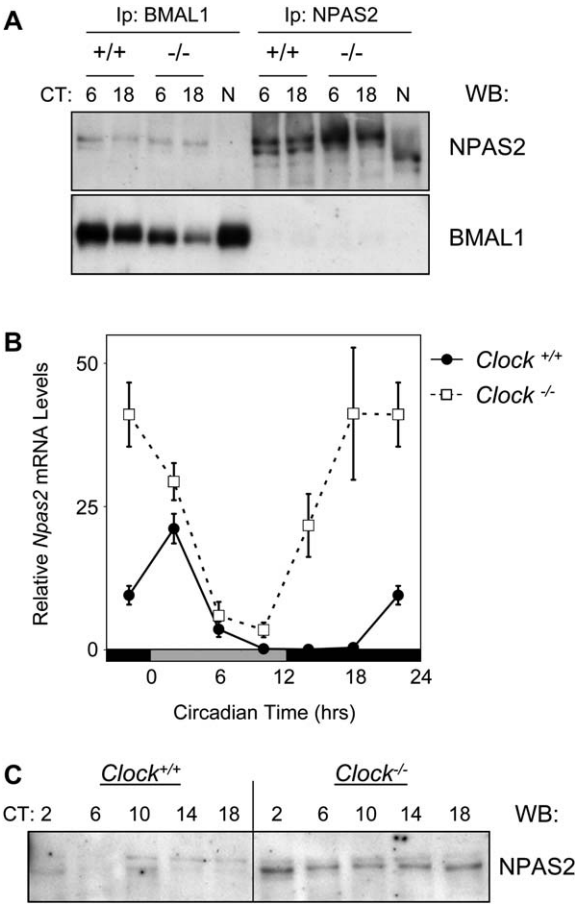

Figure 7. Evaluation of *Npas2* mRNA and Protein Levels in CLOCK-Deficient Mice

(A) BMAL1:NPAS2 interaction in brain. Brains were collected from wild-type (+/+) and CLOCK-deficient (−/−) mice at circadian time (CT) 6 and 18 on the first day in constant darkness. The brains were homogenized and the lysates were immunoprecipitated (Ip) with antibodies against either BMAL1 or NPAS2, and the immune complexes were Western blotted (WB) and probed for either NPAS2 (upper) or BMAL1 (lower). N, brain lysates from $Npas2^{m/m}$ mice. The blots are representative of two independent sets of samples.

(B) Altered *Npas2* mRNA rhythm in the liver of CLOCK-deficient mice. Livers were collected from wild-type mice ($Clock^{+/+}$; solid lines) and CLOCK-deficient mice ($Clock^{-/-}$; dashed lines) at 4 hr intervals on the first day in DD, and the mRNA levels of *Npas2* were determined by quantitative real-time PCR. Each point is the mean ± SEM of three to four animals. The horizontal bar at the bottom of each panel represents the lighting cycle that the animals experienced prior to placement in DD; day is gray, and night is black. Data from CT 22 are double plotted.

(C) NPAS2 levels in liver nuclei. Nuclei were processed from livers collected from wild-type ($Clock^{+/+}$) and homozygous $Clock^{-/-}$ mutant mice at CT 2, 6, 10, 14, and 18 on the first day in constant darkness. The nuclear extracts were Western blotted (WB) and probed for NPAS2. The blot is representative of two experiments, both of which indicate an increase in NPAS2 in the absence of CLOCK.

reprobed these complexes with BMAL1 antibodies (Figure 7A, lower panel) and were able to detect BMAL1 in BMAL1 immune complexes, but not in NPAS2 complexes. The data suggest that BMAL1:NPAS2 interactions can occur in vivo, but the complex may be unstable.

It is noteworthy that *Npas2* mRNA is not detectably expressed in the SCN of wild-type mice by in situ hybridization (Shearman et al., 1999; Dudley et al., 2003). Therefore, if NPAS2 functionally substitutes for CLOCK, we predicted there might be a detectable increase in *Npas2* mRNA levels in the SCN of CLOCK-deficient mice. This was not the case, however. Using in situ hybridization, we could not detect an *Npas2* mRNA signal in the CLOCK-deficient SCN that was greater than the signal produced by the control sense probe (data not shown). Importantly, specific *Npas2* mRNA expression was readily detectable in other brain regions (Zhou et al., 1997; data not shown). These results do not exclude the possibility that *Npas2* is expressed in the SCN at biologically relevant levels, which are below the limit of detection with this approach.

We also examined *Npas2* mRNA levels in the liver in which its circadian expression is apparently regulated by Ror elements within its promoter (Kaasik and Lee, 2004; Ueda et al., 2005). *Npas2* expression was rhythmic, but peaked about 6 hr earlier and at much higher levels in CLOCK-deficient livers compared with wild-type livers (Figure 7B). The altered levels and temporal pattern of *Npas2* mRNA rhythmicity may be due in part to reduced *Rev-erb*α expression in CLOCK-deficient livers (Figure 5A). Furthermore, NPAS2 protein is present at elevated levels in liver nuclear extracts from CLOCK-deficient mice (Figure 7C), suggesting that it may have a role in regulating gene expression in the absence of CLOCK.

Overall, these data are consistent with the possibility that NPAS2 may compensate for the loss of CLOCK. However, analyses of $Clock^{-/-}$; $Npas2^{m/m}$ double mutant mice will be required to test this hypothesis.

Conclusions

Unexpectedly, we found that CLOCK-deficient mice display robust circadian patterns of locomotor activity, with overall period lengths shortened by only ~20 min compared to wild-type. This result was very surprising because homozygous *Clock* mutant mice ($Clock^{\Delta 19/\Delta 19}$) have extraordinarily long circadian periods of behavioral rhythmicity (~27 hr) and substantially damped molecular rhythms (Lowrey and Takahashi, 2004). The mutant CLOCK Δ19 protein still interacts with BMAL1, and this complex can still bind to E box enhancer elements. The transcriptional activity of the mutant CLOCK Δ19 protein is severely compromised (Gekakis et al., 1998; Jin et al., 1999). Moreover, BMAL1-deficient mice lack circadian rhythmicity at both the behavioral and molecular levels (Bunger et al., 2000). Nonetheless, our data indicate that wild-type CLOCK is not required for robust locomotor activity rhythms.

Our data do suggest, however, that CLOCK plays a dominant role in amplifying some molecular rhythms within the SCN and liver. Although the expression of most of the genes examined continues to oscillate in CLOCK-deficient animals, the effects of CLOCK deficiency on gene expression varied considerably. In general, the robustness in the mRNA oscillations of most genes appeared to be more severely disrupted in the liver than in the SCN. For example, there was a modest effect of CLOCK deficiency on the amplitude of the *Rev-erb*α mRNA oscillation in the SCN, while the amplitude of the transcript oscillation was markedly reduced in the liver. The *Dbp* mRNA rhythms, on the other hand, were severely blunted in both the SCN and the liver. Therefore, it appears that the activity of the transcription factors promoting high-amplitude circadian gene expression patterns in the absence of CLOCK are target and tissue specific. It is of interest to note that the less drastic molecular phenotype in the SCN of CLOCK-deficient mice may support a role for intercellular communication in maintaining rhythms in a defective cellular clock (Yamaguchi et al., 2003). Nonetheless, the lack of a consistent molecular phenotype in CLOCK-deficient animals makes it difficult to speculate as to how the specific circadian gene expression patterns contribute to the behavioral phenotype of these mice. The results do suggest, however, that the transcription factor complex supporting circadian gene expression in CLOCK-deficient mice has different specificity compared to CLOCK:BMAL1.

The negative regulators, the mPER and mCRY proteins, appear in the nuclei of CLOCK-deficient SCN and livers at the appropriate time to negatively regulate transcription (Lee et al., 2001). Thus, the negative limb of the circadian clockwork appears to be functional in CLOCK-deficient mice. mBMAL1 is also nuclear in the SCN and liver of CLOCK-deficient mice. BMAL1 is capable of forming homodimers that can bind DNA; however, these homodimers are not transcriptionally active (Rutter et al., 2001). Therefore, the most parsimonious explanation for the persistent rhythmicity in CLOCK-deficient animals is that mBMAL1 is heterodimerizing with another partner and forming a transcriptionally active complex to drive circadian rhythmicity (Figure 8). Further experimentation should shed light on the nature of this CLOCK-independent transcriptional complex. Whether CLOCK deficiency throughout development leads to a molecular compensation mechanism (e.g., upregulation of a BMAL1 partner) to ensure that clock function persists also needs to be assessed. The more severe behavioral and molecular phenotypes of homozygous $Clock^{\Delta 19/\Delta 19}$ mutant mice relative to CLOCK-deficient mice strongly suggests that the mutant CLOCK protein interferes with other transcription factors important for the circadian clock mechanism.

Experimental Procedures

Clock Targeting Construct

The final targeting construct contained *Clock* genomic sequences from nucleotide 67,938 (in intron 3) through 76,584 (in intron 7) of GenBank accession number AF146793, into which a floxed dual Neomycin and thymidine kinase (Neo/TK) cassette was inserted into intron 4, and another *loxP* site was introduced into intron 6 (see Figure 1A).

A probe against the genomic region containing Exon 5 was used to screen a mouse sv129ab genomic library, and a phage clone was isolated. A 10.3 kb EcoRI fragment (nucleotides 67,938–77,667) subcloned into pBluescript SK+ (pSK+, Promega) served as a source of *Clock* genomic fragments, assembled as follows. First, the *LoxP* site from plasmid pBS64 (provided by Dr. Steve

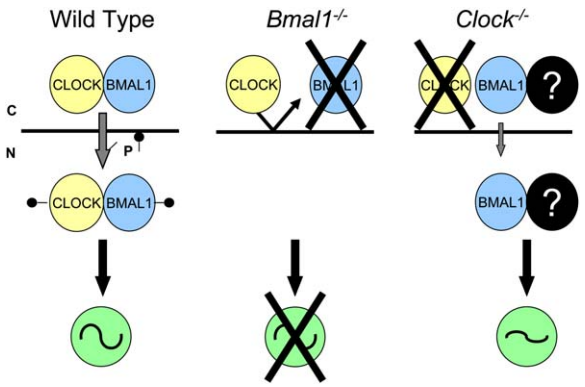

Figure 8. Models of Circadian Transcriptional Activators after Molecular Lesions

In wild-type mice, CLOCK and BMAL1 heterodimerize in the cytoplasm (c), promoting entry into the nucleus (n) (heavy arrow), followed by phosphorylation (p), and activity as a functional transcriptional complex (oscillator sign). In BMAL1-deficient mice (*Bmal*$^{-/-}$), BMAL1 is absent, and CLOCK cannot accumulate in the nucleus (Kondratov et al., 2003). In CLOCK-deficient mice, BMAL1 is able to accumulate in the nucleus, although less efficiently (thin arrow). BMAL1 may heterodimerize in the cytoplasm with another member of the bHLH-PAS family (?) and enter the nucleus to promote transcription. Due to differences in activator/promoter specificity, the ?:BMAL1 complex does not rhythmically activate all genes normally regulated by CLOCK:BMAL1 (damped oscillation sign).

Jones; Albuin and Bradley, 1996; Sauer et al., 1987) was subcloned into pSK+, and a 3.3 kb EcoRV fragment (nucleotides 73,297–76,584) was inserted 3′ to this *LoxP* site to generate the 3′ arm. Adaptor oligos containing BstXI and PmlI sites were ligated 5′ to this *LoxP* site to facilitate further manipulations. Next, a BstXI fragment containing the 5′ arm sequences from 67,938 to 72,246 was ligated into the added *Bst*XI site, producing a plasmid with the flanking 5′ and 3′ arms but lacking the central region including exons 5 and 6. To complete the targeting construct, the sequence from 72,246 to 73,297 (BstXI and EcoRV sites, respectively) was amplified by PCR and cloned into pCRII (Invitrogen) vector and sequenced to verify PCR fidelity. This insert was digested out with EcoRI, inserted into pSK+, digested with BstXI and subcloned into the plasmid pNTL containing the floxed Neo/TK cassette (provided by Dr. Steve Jones) (Albuin and Bradley, 1996). Finally, this floxed Neo/TK-*Clock* fragment was freed from its vector using ClaI, and ligated into the PmlI site created in the construct above, completing the targeting construct. The ligated junctions and *loxP* sites were sequenced to ensure correct assembly, orientation, and sequence.

Generation of Mice Containing *Clock*^{flox} and *Clock*$^{\Delta 5\text{-}6}$ Alleles

The targeting construct was digested out of the pSK+ backbone using *Cla*I, and submitted to the Transgenic Animal Modeling core facility at UMass Medical School for electroporation into strain sv129 ES cells. All ES cell manipulations were carried out by this facility using standard protocols. G418-resistant clones were screened by Southern blot using a probe 3′ of the targeting construct. Clones with a hybridization pattern consistent with homologous recombination of the targeting construct were further characterized by Southern blotting using each of five enzymes that gave unique restriction patterns, using the 3′ flanking and internal probes. Ultimately, two clones were selected and transfected with a P1 bacteriophage *Cre* expression plasmid to promote recombination between *LoxP* sites. The gancyclovir-resistant subclones were screened to distinguish those with recombination between the first and third *LoxP* sites (leading to excision of the Neo/TK cassette and exons 5 and 6) from the desired subclones in which only the Neo/TK cassette was removed (by recombination between the 5′ and central *LoxP* sites; see Figure 1A). For each clone, PCR was performed with two sets of primers that amplify the sequence containing either the 5′ or 3′ *LoxP* sites (Clock 5 loxF: TGAGCTCAATTGTT GACAGG, Clock 5 loxR: CATGAACTCTGAAGGCAGTGA, Clock 3 loxF2: AGCTGGGGTCTATGCTTCCT, Clock 3 loxR: CGCTGAGAGC CAAGACAAT). Reactions were performed using a touch-down cycling protocol: 95ºC for 2 min, 20 cycles of 95ºC for 30 s, 63ºC (−0.5ºC/cycle) for 60 s, 72ºC for 60 s, then 20 cycles of 95ºC for 30 s, 53ºC for 60 s, and 72ºC for 60 s, followed by a final extension phase at 72ºC for 7 min. Product sizes for the 5′ primer set were ~220 nt for wild-type and ~450 nt for the allele containing the *loxP* site. The product sizes for the 3′ primer set were ~280 nt for wild-type and ~380 nt for the floxed allele containing the *loxP* site. Two subclones were further confirmed by Southern blotting as described above and by long-range PCR with primers flanking the targeting construct (5′F: AGCCTGAGCATTATGGTGGT and 3′R: CTTAAAACAACCAGTTATGAGAATTCCATG, corresponding to nucleotide # 67384-67403 and 77663-77692 of Genbank AF146793, respectively). The TripleMaster PCR system (Eppendorf) was used to amplify an ~10.3 kb product. The product was cloned into a TOPO-TA vector (Invitrogen) for end sequencing and restriction mapping.

ES cells from each of the two confirmed clones were injected into C57BL/6J blastocycts to generate chimeric mice. Chimeras were crossed with C57BL/6J mice to identify those with germline transmission by coat color. All but one pup (of >600) had the recessive black coat color. This one pup received the *Clock*^{flox} allele. Mice were genotyped by PCR using the methods described above to amplify genomic DNA from tail biopsies.

To generate whole-animal disruption of *Clock*, heterozygous *Clock*^{flox} mice were bred to transgenic mice carrying the *PRM1-Cre* transgene (Jackson Labs), and male *Clock*^{flox};*PRM1-Cre* offspring were crossed to C57BL/6J females. PCR to distinguish the wild-type, floxed, and deleted alleles utilized a mixture of three primers: Clock 5F3 (CAGCTTCATTTGAAATCTGCAT), Clock 3 loxF2, and Clock 3 loxR (sequences of these primers are listed above) using the conditions described above (examples are shown in Figure 1B). All of the animals used for our studies were derived from either heterozygote intercrosses or crosses of homozygous males (+/+ or −/−) with heterozygous females. Study animals were backcrossed to the C57BL/6 background for two to four generations. We used balanced ratios of both male and female mice in all studies. Animal studies were approved by the Institutional Animal Care and Use Committee of the University of Massachusetts Medical School.

Behavioral Analysis

Mice for behavioral analysis were housed individually in cages equipped with running wheels and maintained in light-tight, ventilated closets within a temperature- and humidity-controlled facility. Food and water were available ad libitum. The animals were maintained on a 12 hr light:12 hr dark (LD) lighting cycle before study and for the first 2 weeks of activity monitoring. Lighting conditions were subsequently manipulated as illustrated (Figures 3 and 4). White light was emitted from fluorescent bulbs controlled by a timer, and dim red light (>600 nm) was present continuously. Running wheels were equipped with magnets on opposing sides, and activity was detected as switch closures using a magnetic reed switch mounted on top of each cage. ClockLab Data Collection (Actimetrics) software monitored and stored activity in 1 min bins. ClockLab Data Analysis software was used to produce the double-plotted actograms as well as for periodogram and phase-shift analyses. χ^2 periodogram analysis was performed using 28 days of data in DD. To measure circadian phase responses to delaying the time of lights-off, linear regressions were fit through the activity onsets for the 10 days before and after release into DD, and the phase shift was measured as the difference in extrapolated onset of activity on the day of the manipulation. Responses to advancing lights-on were measured similarly, except the first 4 days after the lighting manipulation were excluded to avoid "transients." Paired t tests or ANOVA with the Sheffe's S post hoc test were used, with significance levels set at $p \leq 0.05$.

Analysis of Gene Expression

To measure mRNA rhythms in the SCN and liver, tissues were collected at 4 hr intervals on the first day in DD (dim red light). Tissues were collected from four animals per genotype at CT 2, 6, 10, 14, 18, and 22, where CT 0 is the time of lights-on had the animals remained

in an LD cycle. Mice were euthanized by CO_2 inhalation and decapitated. Brains were frozen in 2-methylbutane at ~ −20ºC and stored at −80ºC until processing. A small portion of each liver was frozen on dry ice and kept at −80ºC for analysis of mRNA levels. The rest of the liver was pooled (n = 4 livers in one pool per time point) with others of the same genotype for preparation of purified nuclei as described in Lee et al., 2001.

Gene expression in the SCN was assessed using semiquantitative in situ hybridization as described previously (Jin et al., 1999). Templates for probe generation were identical to those reported elsewhere (*mPer1*, *mPer2*, *Avp*, and *Bmal1*: Jin et al., 1999; *Npas2*: Shearman et al., 1999; *Dbp*: Ripperger et al., 2000; *Pk2*: Cheng et al., 2002; *Rev-erbα*: Onishi et al., 2002).

For analysis of mRNA levels in the liver, quantitative real-time PCR was performed using TaqMan probes with an ABI SDS 7000 instrument (Applied Biosystems, Foster City, CA). Total RNA was extracted using Trizol (Invitrogen), treated with RQ1 DNase (Promega), and random hexamers (Promega) were used to prime reverse-transcription reactions with Superscript II (Invitrogen) using protocols from the manufacturers. PCR reactions were assembled by combining two master mixes in PCR plates. The first contained 0.2–0.5 μl of cDNA template and 13 μl Platinum Quantitative PCR SuperMix-UDG with ROX (Invitrogen) per reaction. The second mix contained primers, probe, and the water needed to bring each reaction to a final volume of 25 μl. Final primer and probe concentrations were 0.9 μM each and 0.25 μM, respectively. The *mPer2*, *mCry2*, *Rev-erbα*, and *Gapdh* primers and probes were identical to those reported by Preitner et al. (2002). The *mPer1* and *Dbp* primers and probes were the same as those used by Wisor et al. (2002) (F = forward primer, R = reverse primer, P = probe, all 5′–3′): *mPer1*F: CAGCTGGGCCGG TTTTG, *mPer1*R: CACTTTATGGCGACCCAACA *mPer1*P: FAM-CACCCCTGGAGCCGCAAGGTG-TAMRA, *Dbp*F: GCCCACCTGGTA CAGAAGGA, *Dbp*R: TCAAGCAGCTGTCTCTTTGCA.

*Dbp*P: FAM-CGCGCGCCTGTGTCCCTTG-TAMRA. The other primers and probes were: *Bmal1F*: ACAACGAGGGCTGCAACCT, *Bmal1R*: CCCGTTCGCTGGTTGTG, *Bmal1P*: FAM-AGCTGCCTCG TTGCA-MGB, *mCry1F*: GCATCAACAGGTGGCGATTT, *mCry1R*: TAATTTTCGTAGATTGGCATCAAGA, *mCry1P*: FAM-TCCTCAAGACA CTGAAGCA-MGB, *Npas2F*: ATGTGTGTAGCTGACGAACCTTTAGA, *Npas2R*: ATGATTGGAGGAGCTCTGTGATC, *Npas2P*: FAM-TCACT TCGAGGCATAGCTTGGAATGGA-TAMRA. All primers and FAM-TAMRA-labeled probes were purchased from Integrated DNA Technologies (Coralville, IA). FAM-MGB-labeled probes were purchased from Applied Biosystems (Foster City, CA). Efficiency of amplification and detection by all primer and probe sets was validated by determining the slope of Ct versus dilution on a 10^5 dilution series. Separate reactions were used to quantify each transcript in a given cDNA sample. Duplicate reactions from each sample were processed together and averaged. Data for each transcript were normalized to *Gapdh* as an internal control using the $2^{-\Delta\Delta Ct}$ method. The average expression level in wild-type mice across time was set to 1.0 to allow direct comparision of transcript levels across genotypes and times. Rhythm amplitude is defined as the fold change between mean peak and trough levels for a given transcript.

Immunoprecipitation and Western Blotting

Purified liver nuclei were isolated as described (Lee et al., 2001). Brains from wild-type and CLOCK-deficient mice were collected at the indicated times on the first day in DD and were bisected in the sagittal plane. Brains from *Npas2* mutant mice (Garcia et al., 2000) were collected during mid-day from animals maintained on a 12:12 LD cycle and were generously provided by S.J. Estill and S.L. McKnight. Lysates from a single brain hemisphere or an aliquot of liver nuclei were immunoprecipitated as described previously (Lee et al., 2001). Antibodies used for immunoprecipitation included CLOCK and BMAL1 antibodies (CLK-1-GP and BM1-2-GP; characterized in Lee et al., 2001). NPAS2 antibodies were generated in guinea pigs or rats (NPAS-GP and NPAS-R) using amino acids 695–817 of GenBank accession NM_008719 as the immunogen (C. Lee and S.M.R., unpublished data). Negative control IPs (using IgG) were performed in parallel for each experiment. Protein lysates or immune complexes were separated on 4%–15% gradient SDS polyacrylamide gels (BioRad) for Western blotting using standard protocols. Primary antibodies used to detect CLOCK, BMAL1, and NPAS2 in immune complexes were CLK-1-R, BM1-2-R, and NPAS2-R, respectively. Primary antibodies to detect proteins from liver nuclear lysates were CLK-1-GP, BM1-2-GP, NPAS2-R, mPER1-1-GP, mPER2-1-R, mCRY1-R (C1-R), and mCRY2-R (C2-R) antibodies, as described previously (Lee et al., 2001, 2004).

Immunocytochemistry

Mice were euthanized on the first day in DD under dim red light by pentobarbital overdose followed by transcardial perfusion fixation. Mice were perfused with 0.01 M phosphate-buffered saline (pH 7.4) followed by 4% paraformaldehyde in 0.1 M phosphate buffer (pH 7.4). Brains were removed, postfixed for 3–5 hr, and then transferred to 0.1 M phosphate buffer in 0.9% saline at room temperature for 2–3 days while in transit. After cryoprotection in 20% sucrose, brains were sectioned at 30 μm on a freezing microtome, and free-floating sections were processed for immunostaining as described previously (Hastings et al., 1999). For each antigen, the antibodies and dilutions used for the experiments shown in Figures 2 and 5 were CLOCK (CLK-1-GP, 1:1000, Lee et al., 2001), BMAL1 (BM1-2-GP, 1:2000; Lee et al., 2001), mPER1 (rabbit 1177, 1:8000; Hastings et al., 1999), mPER2 (mPER2-1-GP, 1:4000; Lee et al., 2001), mCRY1 (C1-GP,1:1000; Lee et al., 2004). Immunoreactivity was visualized by avidin-biotin-peroxidase with the diaminobenzidine chromogen (Vector Labs, Petersborough, UK), and the number of SCN cells with nuclear immunoreactivity was counted using an image analysis system described previously (Hastings et al., 1999) by an observer blind to genotype.

Supplemental Data

The Supplemental Data for this article can be found online at http://www.neuron.org/cgi/content/full/50/3/465/DC1/.

Acknowledgments

We thank Stephen N. Jones and the staff of the Transgenic Animal Modeling facility for assistance, advice, and reagents; Choogon Lee for generating the anti-NPAS2 antibody; Sandi Jo Estill and Steven L. McKnight for providing tissue from *Npas2* mutant mice; and Jean-Pierre Etchegaray and Kaz Machida for assistance with preliminary studies. This work was supported by NIH grants R01 NS047141 (S.M.R.); R21 NS051458 (D.R.W.); and the MRC (E.S.M.). J.P.D. was supported in part by NIH NRSA F32 GM074277, and E.N. was supported by a long-term fellowship from the Human Frontier Science Program. The UMMS Transgenic Animal Modeling facility is supported in part by Diabetes and Endocrinology Research Center grant DK32520.

Received: February 3, 2006
Revised: March 21, 2006
Accepted: March 28, 2006
Published: May 3, 2006

References

Akashi, M., and Takumi, T. (2005). The orphan nuclear receptor RORalpha regulates circadian transcription of the mammalian core-clock Bmal1. Nat. Struct. Mol. Biol. *12*, 441–448.

Albuin, A., and Bradley, A. (1996). Recycling selectable markers in mouse embryonic stem cells. Mol. Cell. Biol. *16*, 1851–1856.

Antoch, M.P., Song, E.-J., Chang, A.-M., Vitaterna, M.H., Zhao, Y., Wilsbacher, L.D., Sangoram, A.M., King, D.P., Pinto, L.H., and Takahashi, J.S. (1997). Functional identification of the mouse circadian *Clock* gene by transgenic BAC rescue. Cell *89*, 655–667.

Bunger, M.K., Wilsbacher, L.D., Moran, S.M., Clendinin, C., Radcliffe, L.A., Hogenesch, J.B., Simon, M.C., Takahashi, J.S., and Bradfield, C.A. (2000). *Mop3* is an essential component of the master circadian pacemaker in mammals. Cell *103*, 1009–1017.

Cheng, M.Y., Bullock, C.M., Li, C., Lee, A.G., Bermak, J.C., Belluzzi, J., Weaver, D.R., Leslie, F.M., and Zhou, Q.-Y. (2002). Prokineticin 2 transmits the behavioral circadian rhythm of the suprachiasmatic nucleus. Nature *417*, 405–410.

Dudley, C.A., Erbel-Sieler, C., Estill, S.J., Reick, M., Franken, P., Pitts, S., and McKnight, S.L. (2003). Altered patterns of sleep and behavioral adaptability in NPAS2-deficient mice. Science *301*, 379–383.

Duffield, G.E. (2003). DNA microarray analyses of circadian timing: the genomic basis of biological time. J. Neuroendocrinol. *15*, 991–1002.

Dunlap, J.C. (1999). Molecular bases for circadian clocks. Cell *96*, 271–290.

Emery, P., and Reppert, S.M. (2004). A rhythmic ror. Neuron *43*, 443–444.

Etchegaray, J.P., Lee, C., Wade, P.A., and Reppert, S.M. (2003). Rhythmic histone acetylation underlies transcription in the mammalian circadian clock. Nature *421*, 177–182.

Field, M.D., Maywood, E.S., O'Brien, J.A., Weaver, D.R., Reppert, S.M., and Hastings, M.H. (2000). Analysis of clock proteins in the mouse SCN demonstrates phylogenetic divergence of the circadian clockwork and resetting mechanisms. Neuron *25*, 437–447.

Garcia, J.A., Zhang, D., Estill, S.J., Michnoff, C., Rutter, J., Reick, M., Scott, K., Diaz-Arrastia, R., and McKnight, S.L. (2000). Impaired cued and contextual memory in NPAS2-deficient mice. Science *288*, 2226–2230.

Gekakis, N., Staknis, D., Nguyen, H.B., Davis, F.C., Wilsbacher, L.D., King, D.P., Takahashi, J.S., and Weitz, C.J. (1998). Role of CLOCK protein in the mammalian circadian mechanism. Science *280*, 1564–1569.

Hastings, M.H., Field, M.D., Maywood, E.S., Weaver, D.R., and Reppert, S.M. (1999). Differential regulation of mPER1 and mTIM proteins in the mouse suprachiasmatic nuclei: new insights into a core clock mechanism. J. Neurosci. *19*, 1–7.

Hogenesch, J.B., Chan, W.K., Jackiw, V.H., Brown, R.C., Gu, Y.Z., Pray-Grant, M., Perdew, G.H., and Bradfield, C.A. (1997). Characterization of a subset of the basic-helix-loop-helix-PAS superfamily that interacts with components of the dioxin signaling pathway. J. Biol. Chem. *272*, 8581–8593.

Hogenesch, J.B., Gu, W.Z., Jain, S., and Bradfield, C.A. (1998). The basic-helix-loop-helix-PAS orphan MOP3 forms transcriptionally active complexes with circadian and hypoxia factors. Proc. Natl. Acad. Sci. USA *95*, 5474–5479.

Jin, X., Shearman, L.P., Weaver, D.R., Zylka, M.J., De Vries, G.J., and Reppert, S.M. (1999). A molecular mechanism regulating rhythmic output from the suprachiasmatic circadian clock. Cell *96*, 57–68.

Kaasik, K., and Lee, C.C. (2004). Reciprocal regulation of haem biosynthesis and the circadian clock in mammals. Nature *430*, 467–471.

Kennaway, D.J., Voultsios, A., Varcoe, T.J., and Moyer, R.W. (2003). Melatonin and activity rhythm responses to light pulses in mice with the *Clock* mutation. Am. J. Physiol. *284*, R1231–R1240.

King, D.P., Vitaterna, M.H., Chang, A.-M., Dove, W.F., Pinto, L.H., Turek, F.W., and Takahashi, J.S. (1997a). The mouse *Clock* mutation behaves as an antimorph and maps within the W^{19H} deletion, distal of *kit*. Genetics *146*, 1049–1060.

King, D.P., Zhao, Y., Sangoram, A.M., Wilsbacher, L.D., Tanaka, M., Antoch, M.P., Steeves, T.D., Vitaterna, M.H., Kornhauser, J.M., Lowrey, P.L., et al. (1997b). Positional cloning of the mouse circadian *Clock* gene. Cell *89*, 641–653.

Kondratov, R.V., Chernov, M.V., Kondratova, A.A., Gorbacheva, V.Y., Gudkov, A.V., and Antoch, M.P. (2003). BMAL1-dependent circadian oscillation of nuclear CLOCK: posttranslational events induced by the dimerization of the transcriptional activators of the mammalian clock system. Genes Dev. *17*, 1921–1932.

Kume, K., Zylka, M.J., Sriram, S., Shearman, L.P., Weaver, D.R., Jin, X., Maywood, E.S., Hastings, M.H., and Reppert, S.M. (1999). mCRY1 and mCRY2 are essential components of the negative limb of the circadian clock feedback loop. Cell *98*, 193–205.

Lee, C., Etchegaray, J.P., Cagampang, F.R., Loudon, A.S., and Reppert, S.M. (2001). Posttranslational mechanisms regulate the mammalian circadian clock. Cell *107*, 855–867.

Lee, C., Weaver, D.R., and Reppert, S.M. (2004). Direct association between mouse PERIOD and CKIepsilon is critical for a functioning circadian clock. Mol. Cell. Biol. *24*, 584–594.

Lowrey, P.L., and Takahashi, J.S. (2004). Mammalian circadian biology: elucidating genome-wide levels of temporal organization. Annu. Rev. Genomics Hum. Genet. *5*, 407–441.

Lowrey, P.L., Shimomura, Z., Antoch, M.P., Yamazaki, S., Zemenideds, P.D., Ralph, M.R., Menaker, M., and Takahashi, J.S. (2000). Positional syntenic cloning and functional characterization of a mammalian circadian mutation *tau*. Science *288*, 483–491.

McNamara, P., Seo, S., Rudic, R.D., Sehgal, A., Chakravarti, D., and FitzGerald, G.A. (2001). Regulation of CLOCK and MOP4 by nuclear hormone receptors in the vasculature: a humoral mechanism to reset a peripheral clock. Cell *105*, 877–889.

Morozov, A., Kellendonk, C., Simpson, E., and Tronche, F. (2003). Using conditional mutagenesis to study the brain. Biol. Psychiatry *54*, 1125–1133.

Nagoshi, E., Saini, C., Bauer, C., Laroche, T., Naef, F., and Schibler, U. (2004). Circadian gene expression in individual fibroblasts: cell-autonomous and self-sustained oscillators pass time to daughter cells. Cell *119*, 693–705.

Nagy, A. (2000). Cre recombinase: the universal reagent for genome tailoring. Genesis *26*, 99–109.

Ochi, M., Sono, S., Sei, H., Oishi, K., Kobayashi, H., Morita, Y., and Ishida, N. (2003). Sex difference in circadian period of body temperature in Clock mutant mice with Jcl/ICR background. Neurosci. Lett. *347*, 163–166.

O'Gorman, S., Dagenais, N.A., Qian, M., and Marchuk, Y. (1997). Protamine-Cre recombinase transgenes efficiently recombine target sequence in the male germ line of mice, but not in embryonic stem cells. Proc. Natl. Acad. Sci. USA *94*, 14602–14607.

Oishi, K., Fukui, H., and Ishida, N. (2000). Rhythmic expression of *BMAL1* mRNA is altered in *Clock* mutant mice: differential regulation in the suprachiasmatic nucleus and peripheral tissues. Biochem. Biophys. Res. Commun. *268*, 164–171.

Oishi, K., Miyazaki, K., and Ishida, N. (2002). Functional CLOCK is not involved in the entrainment of peripheral clocks to the restricted feeding: entrainable expression of *mPer2* and *BMAL1* mRNAs in the heart of *Clock* mutant mice on Jcl:ICR background. Biochem. Biophys. Res. Commun. *298*, 198–202.

Onishi, H., Yamaguchi, S., Yagita, K., Ishida, Y., Dong, X., Kimura, H., Jing, Z., Ohara, H., and Okamura, H. (2002). Rev-erbα gene expression in the mouse brain with special emphasis on its circadian profiles in the suprachiasmatic nucleus. J. Neurosci. Res. *68*, 551–557.

Preitner, N., Damiola, F., Lopez-Molina, L., Zakany, J., Duboule, D., Albrecht, U., and Schibler, U. (2002). The orphan nuclear receptor REV-ERBα controls circadian transcription within the positive limb of the mammalian circadian oscillator. Cell *110*, 251–260.

Redlin, U., Hattar, S., and Mrosovsky, N. (2005). The circadian *Clock* mutant mouse: impaired masking response to light. J. Comp. Physiol. [A] *191*, 51–59.

Reppert, S.M., and Weaver, D.R. (2002). Coordination of circadian timing in mammals. Nature *418*, 935–941.

Reick, M., Garcia, J.A., Dudley, C., and McKnight, S.L. (2001). NPAS2: an analog of Clock operative in the mammalian forebrain. Science *293*, 506–509.

Ripperger, J.A., Shearman, L.P., Reppert, S.M., and Schibler, U. (2000). CLOCK, an essential pacemaker component, controls expression of the circadian transcription factor DBP. Genes Dev. *14*, 679–689.

Rutter, J., Reick, M., Wu, L.C., and McKnight, S.L. (2001). Regulation of CLOCK and NPAS2 DNA binding by the redox state of NAD cofactors. Science *293*, 510–514.

Sato, T.K., Panda, S., Miraglia, L.J., Reyes, T.M., Rudic, R.D., McNamara, P., Naik, K.A., FitzGerald, G.A., Kay, S.A., and Hogenesch, J.B. (2004). A functional genomics strategy reveals Rora as a component of the mammalian circadian clock. Neuron *43*, 527–537.

Sauer, B., Whealy, M., Robbins, A., and Enquist, L. (1987). Site-specific insertion of DNA into a pseudorabies virus vector. Proc. Natl. Acad. Sci. USA *84*, 9108–9112.

Shearman, L.P., Zylka, M.J., Reppert, S.M., and Weaver, D.R. (1999). Expression of basic helix-loop-helix/PAS genes in the mouse suprachiasmatic nucleus. Neuroscience *89*, 387–397.

Shearman, L.P., Sriram, S., Weaver, D.R., Maywood, E.S., Chaves, I., Zheng, B., Kume, K., Lee, C.C., van der Horst, G.T.J., Hastings, M.H., and Reppert, S.M. (2000). Interacting molecular loops within the mammalian circadian clock. Science *288*, 1013–1019.

Ueda, H.R., Chen, W., Adachi, A., Wakamatsu, H., Hayashi, S., Takasugi, T., Nagano, M., Nakahama, K., Suzuki, Y., Sugano, S., et al. (2002). A transcription factor response element for gene expression during the circadian night. Nature *418*, 534–539.

Ueda, H.R., Hayashi, S., Chen, W., Sano, M., Machida, M., Shigeyoshi, Y., Iino, M., and Hashimoto, S. (2005). System-level identification of transcriptional circuits underlying mammalian circadian clocks. Nat. Genet. *37*, 187–192.

Vitaterna, M.H., King, D.P., Chang, A.-M., Kornhauser, J.M., Lowrey, P.L., McDonald, J.D., Dove, W.F., Pinto, L.H., Turek, F.W., and Takahashi, J.S. (1994). Mutagenesis and mapping of a mouse gene, *Clock*, essential for circadian behavior. Science *264*, 719–725.

Welsh, D.K., Yoo, S.H., Liu, A.C., Takahashi, J.S., and Kay, S.A. (2005). Bioluminescence imaging of individual fibroblasts reveals persistent, independently phased circadian rhythms of clock gene expression. Curr. Biol. *14*, 2289–2295.

Winfree, A.T. (1970). Integrated view of resetting a circadian clock. J. Theor. Biol. *28*, 327–374.

Wisor, J.P., O'Hara, B.F., Terao, A., Selby, C.P., Kilduff, T.S., Sancar, A., Edgar, D.M., and Franken, P. (2002). A role for cryptochromes in sleep regulation. BMC Neurosci. *3*, 20.

Yamaguchi, S., Isejima, H., Matsuo, T., Okura, R., Yagita, K., Kobayashi, M., and Okamura, H. (2003). Synchronization of cellular clocks in the suprachiasmatic nucleus. Science *302*, 1408–1412.

Yoo, S.H., Ko, C.H., Lowrey, P.L., Buhr, E.D., Song, E.J., Chang, S., Yoo, O.J., Yamazaki, S., Lee, C., and Takahashi, J.S. (2005). A noncanonical E-box enhancer drives mouse Period2 circadian oscillations in vivo. Proc. Natl. Acad. Sci. USA *102*, 2608–2613.

Zhou, Y.-D., Barnard, M., Tian, H., Li, X., Ring, H.Z., Francke, U., Shelton, J., Richardson, J., Russell, D.W., and McKnight, S.L. (1997). Molecular characterization of two mammalian bHLH-PAS domain proteins selectively expressed in the central nervous system. Proc. Natl. Acad. Sci. USA *94*, 713–718.